

## Structure and Kinetics of the $\beta$ -Lactamase Mutants S70A and K73H from *Staphylococcus aureus* PC1<sup>†,‡</sup>

Celia C. Chen,<sup>§</sup> Tom J. Smith,<sup>§,||,⊥</sup> Geeta Kapadia,<sup>§</sup> Susana Wäsch,<sup>§</sup> Laura E. Zawadzke,<sup>§</sup> Andrew Coulson,<sup>||</sup> and Osnat Herzberg<sup>\*,§</sup>

Center for Advanced Research in Biotechnology, University of Maryland Biotechnology Institute, 9600 Gudelsky Drive, Rockville, Maryland 20850, and Institute for Cell and Molecular Biology, University of Edinburgh, King's Buildings, Mayfield Road, Edinburgh EH9 3JR, U.K.

Received May 15, 1996; Revised Manuscript Received July 18, 1996<sup>⊗</sup>

**ABSTRACT:** Two mutant  $\beta$ -lactamases from *Staphylococcus aureus* PC1 which probe key catalytic residues have been produced by site-directed mutagenesis. In the S70A enzyme, the nucleophilic group that attacks the  $\beta$ -lactam carbonyl carbon atom was eliminated. Consequently, the  $k_{\text{cat}}$  values for hydrolysis of benzylpenicillin and nitrocefin have been reduced by  $10^4$ – $10^5$  compared with the wild-type enzyme. The crystal structure of S70A  $\beta$ -lactamase has been determined at 2.1 Å resolution. With the exception of the mutation site, the structure is identical to that of the native enzyme. The residual activity is attributed either to mistranslation that leads to production of wild-type enzyme and/or to remaining features of the active site that stabilize the tetrahedral transition state. Soaking of the crystals with ampicillin or clavulanate, followed by flash-freezing, has been carried out and the structures examined at 2.0 Å resolution. For both experiments, the difference electron density maps revealed buildup of density in the active site that presumably corresponds to  $\beta$ -lactam binding. However, neither electron density is sufficiently clear for defining the atomic details of the bound compounds. The K73H  $\beta$ -lactamase has been prepared to test the possible role of Lys73 in proton transfer. It exhibits no detectable activity toward benzylpenicillin, and  $10^5$ -fold reduction of  $k_{\text{cat}}$  for nitrocefin hydrolysis compared with the wild-type enzyme. No significant recovery of activity has been measured when the pH was varied between 5.0 and 8.0. The crystal structure of K73H  $\beta$ -lactamase has been determined at 1.9 Å resolution. While the overall structure is similar to that of the native enzyme, the electrostatic interactions between His73 and neighboring residues indicate that the imidazole ring is positively charged. In addition, the hydroxyl group of Ser70 adopts a position that is incompatible with nucleophilic attack on substrates. A crystal soaked with ampicillin was flash-frozen, and diffraction data were collected at 2.1 Å resolution. The electron density map showed no indication of substrate binding.

The class A  $\beta$ -lactamases hydrolyze  $\beta$ -lactam antibiotics by a mechanism that involves a nucleophilic attack of a serine hydroxyl group, Ser70, on the carbonyl carbon atom of the  $\beta$ -lactam bond [the consensus numbering scheme according to Ambler et al. (1991) will be used throughout]. Biochemical data indicate that the reaction progresses via a seryl acyl-enzyme intermediate (Coulson, 1985; Knowles, 1985), a mechanism that is reminiscent of that of the serine proteases. Several high-resolution crystal structures of class A  $\beta$ -lactamases have been determined (Herzberg & Moulton, 1987; Herzberg, 1991; Moews et al., 1990; Knox & Moews, 1991; Jelsch et al., 1992, 1993; Strynadka et al., 1992). All show that Ser70 is located at the bottom of a rather shallow

depression that constitutes the active site. Similarly to the serine proteases, the assisting catalytic machinery includes an oxyanion hole that helps stabilize the negatively-charged tetrahedral transition state. A lysine residue (Lys73) is located in an analogous position to that of the catalytic histidine in the serine proteases (Herzberg & Moulton, 1987). Following this analogy, the authors discussed two alternative mechanisms by which Lys73 could assist the acylation step. In the first, the lysine side-chain accepts a proton from the catalytic serine hydroxyl group and transfers it to the nitrogen atom of the  $\beta$ -lactam amide in a manner similar to that proposed for the catalytic histidine residue in the serine proteases. This mechanism implies that the lysine is uncharged. The second mechanism invokes a positively charged lysine which could provide a potential gradient for a direct proton transfer from Ser70 to the substrate.

In contrast to the analogy between the histidine residue of the serine proteases and the lysine residue of the  $\beta$ -lactamases, Ofner et al. (1990) and Lobkovsky et al. (1994) observed that the hydroxyl group of Ser130 in the class A  $\beta$ -lactamases and its counterpart, the Tyr150 hydroxyl in the related class C enzymes, fit better the position of the catalytic histidine of the serine proteases. They concluded that at least for the class C  $\beta$ -lactamases, Tyr150 is the general base in

<sup>†</sup> Supported by NIH Grant RO1-AI27175. T.J.S. acknowledges a research studentship from the Medical Research Council.

<sup>‡</sup> The coordinates of the crystal structures of S70A and K73H mutant  $\beta$ -lactamases, determined at room temperature, and of S70A mutant enzyme, determined at approximately 120 K, have been deposited in the Brookhaven Protein Data Bank. Entry codes are 1DJB, 1DJA, and 1DJC, respectively.

<sup>\*</sup> To whom correspondence should be addressed. Telephone: 301-738-6245. Fax: 301-738-6255. E-mail: osnat@elan1.carb.nist.go.

<sup>§</sup> University of Maryland Biotechnology Institute.

<sup>||</sup> University of Edinburgh.

<sup>⊥</sup> Present address: Department of Molecular Biology and Biotechnology, University of Sheffield, P.O. Box 594, Firth Court, Western Bank, Sheffield S10 2UH, U.K.

<sup>⊗</sup> Abstract published in *Advance ACS Abstracts*, September 1, 1996.

acylation and deacylation and thus the lysine residue does not have a role in assisting proton transfer. Another proposal that has been advanced is that neither the lysine nor Ser130 of the class A  $\beta$ -lactamases assists proton transfer during acylation; rather, Glu166 plays this role (Gibson et al., 1990; Lamotte-Brasseur, 1991). Finally, Strynadka et al. (1992) proposed that Lys73 is uncharged and that both Lys73 and Ser130 concomitantly assist proton transfer. Clearly, knowledge of the  $pK_a$  of the lysine residue is crucial for resolving this controversy. Recent NMR studies which undertook to assign the  $^1\text{H}$  and  $^{13}\text{C}$  chemical shifts of Lys73 and their pH dependence suggested that the residue is positively charged in the free enzyme, with a  $pK_a$  value above 10 (Dambon et al., 1996). The data have been taken as proof that Glu166 rather than Lys73 is the general base during both acylation and deacylation reactions. On the other hand, computational electrostatic analysis indicated that the  $pK_a$  of Lys73 is 8 (Swarén et al., 1995). These calculations should be considered with caution because of the sensitivity of the results to the value of the protein dielectric constant. A protein dielectric constant of 3 was assumed here. However, it has been shown that the experimental  $pK_a$  values of ionizable groups in proteins are not well reproduced when such a low dielectric constant is used, whereas the use of a much higher dielectric constant of 20 leads to closer agreement with the experimental data (Antosiewicz et al., 1994).

While the deacylating water in the serine proteases has been proposed to bind upon departure of the leaving group, replacing the nitrogen atom of the cleaved peptide, evidence has accumulated that in the class A  $\beta$ -lactamases the deacylating water attacks from the opposite direction. All class A  $\beta$ -lactamases whose crystal structures have been determined contain a water molecule that forms electrostatic interactions with the invariant Ser70, Glu166, and Asn170. It has been proposed that Glu166 enhances the nucleophilicity of this water molecule (Herzberg & Moul, 1987, 1991). Indeed, in the P54 mutant enzyme from *Staphylococcus aureus* PC1, Glu166 is conformationally disordered, and deacylation becomes the rate-limiting step (Herzberg et al., 1991). In the *Escherichia coli* TEM-1 and *Bacillus licheniformis*  $\beta$ -lactamases, replacement of Glu166 by a noncharged residue resulted in accumulation of the acyl-enzyme intermediate (Adachi et al., 1991; Escobar et al., 1991). One of these mutant enzymes (E166N) was used to determine the crystal structure of an acyl-enzyme of the TEM-1  $\beta$ -lactamase (Strynadka et al., 1992). The proposal of Gibson et al. (1990) and Lamotte-Brasseur et al. (1991), implicating Glu166 in both acylation and deacylation steps, is inconsistent with these data.

The availability of a high-resolution structure (Herzberg, 1991) and of an overexpression system (Zawadzke et al., 1995) of the  $\beta$ -lactamase from *S. aureus* PC1 facilitated the current study which investigates the residual activity and structural consequences of mutant enzymes lacking the key catalytic functional groups at positions 70 and 73.

Earlier work, replacing Ser70 of the *Streptomyces albus* G  $\beta$ -lactamase by an alanine, showed that there was a weak residual activity of the mutant enzyme (Jacob et al., 1991). For the *S. aureus*  $\beta$ -lactamase, in addition to determining the extent by which the catalytic activity of the S70A enzyme was abolished, we hoped that the protein would form stable noncovalent complexes with  $\beta$ -lactam compounds which would resemble the Michaelis complexes. If such complexes

were obtained, they could be examined by X-ray crystallography.

For position 73, the activity of the mutant K73R  $\beta$ -lactamase from *Bacillus cereus* was reported to be much impaired (Gibson et al., 1990). Yet, the rate constants for a number of  $\beta$ -lactam antibiotics are not negligible: When compared with the wild-type enzyme, the first-order rate constants of the acylation and deacylation steps for benzylpenicillin decreased by 75-fold and 16-fold, respectively. Similarly, in the class C  $\beta$ -lactamases, which are also serine enzymes with related but not identical catalytic mechanism, replacement of the equivalent lysine residue by an arginine also produced impaired enzyme that exhibited appreciable activity (Tsukamoto et al., 1990; Monnaie et al., 1994). By contrast, replacement by glutamic acid, threonine, or glutamine essentially abolished the catalytic activity. Apparently, an arginine side-chain can mimic the function of a lysine side-chain in either class A or class C  $\beta$ -lactamases. The reduced activity may perhaps be attributed to the larger side-chain of the arginine which partially blocks the approach of the substrate.

The activity of the K73R mutant  $\beta$ -lactamase pertains to the controversy about the protonation state of the lysine in the native protein. The  $pK_a$  of an arginine is higher than that of a lysine; thus, charge-neutralization at physiological pH is less likely to occur. If it could be assumed that the arginine exists predominantly in the charged state, the significant activity that the mutant enzyme exhibits would indicate that the native lysine residue is also charged. In the current study, the K73H mutant enzyme from *S. aureus* has been prepared with the anticipation that it too would be an impaired enzyme. Nevertheless, monitoring the pH dependence of the residual activity could provide information, albeit indirectly, about the  $pK_a$  of Lys73 in the native enzyme. The catalytic activities of the S70A and K73H  $\beta$ -lactamases are drastically reduced. We report here the preparation, kinetic characterization, and X-ray structures of these two mutant enzymes, and the results of binding studies in the crystalline state.

## MATERIALS AND METHODS

*Mutagenesis, Expression, and Protein Purification.* S70A  $\beta$ -lactamase was cloned and expressed in two different host systems, *S. aureus* (Smith, 1992) and *E. coli* (Zawadzke et al., 1995). For easy access, the expression system in *S. aureus* is briefly described below.

The plasmid pWN101 (Wang & Novick, 1987) was used as the source of the *S. aureus*  $\beta$ -lactamase gene and as the basis for the shuttle and expression plasmid pTS6. pWN101 is an *E. coli*-*S. aureus* shuttle plasmid that confers resistance to chloramphenicol and directs expression of secreted staphylococcal  $\beta$ -lactamase in *S. aureus*. The deduced amino acid sequence of the secreted part of the pWN101  $\beta$ -lactamase gene is identical to the amino acid sequence of the *S. aureus* PC1 enzyme (Ambler, 1979).

The shuttle plasmid pTS6 was constructed as follows. pWN101, which has two *Hind*III sites, was cut partially with *Hind*III, and the molecules that had been cut only once were gel-purified. The overlapping ends were polished with the Klenow fragment of *E. coli* DNA polymerase I, and the plasmid was circularized by ligation and transformed into *E. coli* MC1061 (Casadaban & Cohen, 1980). Transformants

were selected with ampicillin (80  $\mu\text{g}/\text{mL}$ ), the progeny were analyzed by restriction digestion with *EcoRI* and *XbaI*, and a clone, pTS4, from which the *HindIII* site further from the  $\beta$ -lactamase gene had been removed, was selected. pTS4 was restricted with *HindIII*, dephosphorylated, and ligated to the 787 bp *HindIII* fragment of pCM7 (Close & Rodriguez, 1982), which contains the Tn9 chloramphenicol acetyltransferase (CAT) gene. The ligation mixture was transformed into *E. coli* MC1061, and transformants containing the plasmid pTS5, in which the Tn9 CAT gene is oriented with its reading frame running in the opposite direction to that of the *S. aureus*  $\beta$ -lactamase gene, were selected with chloramphenicol (20  $\mu\text{g}/\text{mL}$ ). Finally, the *HindIII* site further from the  $\beta$ -lactamase gene in pTS5 was removed by partial cutting and end-filling as above, to give pTS6, which replicates stably in *E. coli* MC1061 and *S. aureus* RN4220 (Kreiswirth et al., 1983). pTS6 confers resistance to ampicillin (80  $\mu\text{g}/\text{mL}$ ) in *E. coli* and resistance to chloramphenicol in *E. coli* and *S. aureus* at 20 and 5  $\mu\text{g}/\text{mL}$ , respectively. In *S. aureus* RN4220, pTS6 directs the production of secreted staphylococcal  $\beta$ -lactamase at about 25% the production level in *S. aureus* PC1.

The S70A mutation was made by the overlap extension polymerase chain reaction (PCR) method (Ho et al., 1989). The external PCR primers were oligonucleotides 164J (5'-CACTCTTGCGGGTTTCAC-3') and 165J (5'-GCATTCATCAGGCGGGC-3'). The internal (mutagenic) primers were oligonucleotides 542C and 163J (5'-CCTATGCTGCAACTTCA-3' and 5'-TTTGAAGTTGCAGCATAGGCA-3', respectively, mismatches underlined).

The final, 1209 bp PCR product was restricted with *HindIII* and *XbaI*, and the largest (840 bp) fragment was gel-purified and ligated into pTS6 that had been cut with the same enzymes and dephosphorylated. The ligation mixture was transformed into *E. coli* MC1061, and transformants were selected using chloramphenicol (20  $\mu\text{g}/\text{mL}$ ). Plasmid DNA from ampicillin-sensitive progeny was used to transform *S. aureus* RN4220; transformants were selected with chloramphenicol (5  $\mu\text{g}/\text{mL}$ ). The frequency of staphylococcal transformation from plasmid DNA from all six ampicillin-sensitive progeny used was much lower than that seen with wild-type pTS6, and almost all the *S. aureus* transformants obtained from using the mutant plasmid contained deleted plasmids or no plasmid at all. Eventually, a single transformant carrying an apparently intact mutant plasmid was isolated. On sequencing, it was found that, in addition to the desired S70A mutation, a single base change (GGAGGG to GAAGGG) had occurred in the Shine-Dalgarno sequence of the  $\beta$ -lactamase gene. This plasmid was termed pTS6.S70A.SD<sup>#</sup>. Thus, the spontaneous SD<sup>#</sup> mutation was exploited to allow the S70A enzyme to be expressed in *S. aureus*, albeit at a rather low level of expression. Using the previously published method (Moult et al., 1985), about 1.5 mg of pure S70A  $\beta$ -lactamase was obtained from 17 L of culture of *S. aureus* RN4220 containing pTS6.S70A.SD<sup>#</sup>. Chloramphenicol (5  $\mu\text{g}/\text{mL}$ ) was added to the medium to maintain selection for the plasmid.

For expression in *E. coli*, the part of the gene encoding the mature secreted protein was amplified by PCR from pTS6.S70A.SD<sup>#</sup> using the oligonucleotide primers TSBSPHI (5'-CAAACAGTTCACTCATGAAAGAGTTAAATGATTTAG-3') and TSHIND3 (5'-ATCAGTTTTTGATAT-

CAAGCTTATACATGTCAACG-3'). The 1387 bp PCR product was cut with *BspHI* and *HindIII*, which cut only within the sequences of oligonucleotides TSBSPHI and TSHIND3, respectively. The PCR product was then gel-purified and ligated into pKK233-2 (Amann & Brosius, 1985) that had been cut with *NcoI* and *HindIII* and dephosphorylated. The ligation mixture was transformed into *E. coli* TG1, and transformants were selected on the basis of resistance to ampicillin (100  $\mu\text{g}/\text{mL}$ ). The resulting plasmid was digested with *HindIII* and *BamHI*; the smaller (1.1 kb) fragment was gel-purified and ligated into pTS32 (Zawadzke et al., 1995). Transformants of *E. coli* TG1 were selected with chloramphenicol (20  $\mu\text{g}/\text{mL}$ ). The resulting plasmid was termed pTS32.S70A, and the correct sequence of the mutant  $\beta$ -lactamase gene was confirmed by DNA sequencing as previously described (Zawadzke et al., 1995).

The K73H  $\beta$ -lactamase was cloned and produced in *E. coli* following the same protocol as in Zawadzke et al. (1995), except that Vent<sub>R</sub> DNA polymerase, purchased from New England Biolab (Beverly, MA), was used for the PCR instead of Taq DNA polymerase. The following oligonucleotides were used as mutagenic primers:

TSK73H1

5'-ATGCTTCAACTTCACACGCGATAAATAGTGC-3'

TSK73H2

5'-GCACTATTTATCGCGTGTGAAGTTGAAGCAT-3'

Protein concentrations were estimated from the absorbance of solutions at 280 nm by using the value of  $\epsilon_{280} = 19\,500\text{ M}^{-1}\text{ cm}^{-1}$  (Carrey & Pain, 1978). For storage, the proteins were kept at 4 °C in solutions containing 60% saturated ammonium sulfate.

**Enzyme Kinetics.** The chromogenic cephalosporin, nitrocefin, was obtained from Unipath (Ogdensburg, NY); benzylpenicillin and ampicillin were purchased from Sigma; lithium clavulanate was purchased from U. S. Pharmacopoeia Convention, Inc. Kinetic measurements were made in a Perkin-Elmer PE320 UV/visible spectrophotometer for the S70A enzyme expressed in *S. aureus*, in a Varian Cary 4 spectrophotometer for the S70A enzyme expressed in *E. coli*, and in a Hewlett Packard 8452A diode array spectrophotometer for the K73H  $\beta$ -lactamase mutant. All assays were performed at 25 °C in 0.1 M potassium phosphate buffer at pH 6.8.

Substrate hydrolysis was monitored by loss of UV absorption for benzylpenicillin ( $\Delta\epsilon_{232} = 940\text{ M}^{-1}\text{ cm}^{-1}$ ) and by the increase in absorbance at 500 nm for nitrocefin ( $\Delta\epsilon_{500} = 15\,900\text{ M}^{-1}\text{ cm}^{-1}$ ).

**Crystallization.** The crystals of the S70A and K73H  $\beta$ -lactamases were grown by the vapor-diffusion method in hanging drops equilibrated at room temperature against reservoir solutions containing 76–78% saturated ammonium sulfate, 0.4% w/v poly(ethylene glycol) 1000, 0.3 M KCl, and 0.1 M NaHCO<sub>3</sub> buffered at pH 8.0. The hanging drops contained approximately 10 mg/mL enzyme solution mixed with an equal volume of the reservoir solution. These are the same conditions used to crystallize the native enzyme (Herzberg & Moult, 1987). The crystals of the S70A mutant enzyme used for structure determination were obtained from protein that was expressed in *S. aureus*, and the same type of crystals was obtained later from protein expressed in *E.*

Table 1: Data Processing Statistics<sup>a</sup>

data set	resolution, Å	cell dimensions, Å	observations, no.	unique reflections, no.	$R_{\text{sym}}^b$	completeness	fraction with $I \geq \sigma(I)$
S70A	2.1	53.7, 93.3, 138.3	63813 (3089)	18843 (1492)	0.092 (0.327)	0.85 (0.45)	0.80 (0.50)
S70A+AmpC	2.0	53.3, 87.4, 139.2	50754 (2702)	19460 (1559)	0.074 (0.206)	0.85 (0.41)	0.87 (0.69)
S70A+Clv	2.0	53.1, 87.5, 139.8	20639 (1278)	15982 (1192)	0.063 (0.254)	0.72 (0.33)	0.86 (0.69)
K73H	1.9	53.9, 93.6, 139.1	61878 (3897)	21589 (1971)	0.067 (0.218)	0.79 (0.44)	0.88 (0.67)
K73H+AmpC	2.1	53.4, 90.7, 140.3	45978 (3011)	17901 (1986)	0.076 (0.273)	0.92 (0.63)	0.85 (0.56)

<sup>a</sup> Abbreviations: AmpC, ampicillin; Clv, clavulanate. The values in parentheses correspond to the highest 0.1 Å resolution shell. <sup>b</sup>  $R_{\text{sym}} = \sum_i \sum_j |I(h)| - I(h)_i / \sum_i \sum_j I(h)_i$  for symmetry-related observations.

*coli*. Crystals of the K73H enzyme were obtained from protein produced in *E. coli*. The crystals of both mutant enzymes belonged to space group *I222* and were isomorphous with those of the native enzyme (Table 1).

**Data Collection and Structure Refinement.** X-ray intensity data were collected on a Siemens area detector mounted on a Siemens 3-circle goniostat. Monochromated CuK $\alpha$  X-rays were generated by a Rigaku Rotaflex RU-200BH rotating anode. Data to 2.0 Å resolution for the S70A  $\beta$ -lactamase and to 1.9 Å resolution for the K73H mutant enzyme were collected at room temperature, each from a single crystal. The data were processed with the XENGEN package (Howard et al., 1987). The statistics of data processing are shown in Table 1.

Structure factors were calculated using the protein coordinates of the native structure (Herzberg, 1991; entry code 3BLM in the Protein Data Bank), initially omitting the mutated residues. The difference electron density maps calculated with the coefficients  $2F_o - F_c$ ,  $F_o - F_c$  (where  $F_o$  and  $F_c$  are the observed and calculated structure factors, respectively) and calculated phases confirmed unambiguously the expected mutations. These residues were then incorporated into the models. The structure of the S70A  $\beta$ -lactamase mutant was refined using the restrained-parameter least-squares method (Hendrickson & Konner, 1980), with the version of the program to which a fast Fourier transform calculation has been added (Finzel, 1987). The refinement was completed using the positional refinement protocol of X-PLOR (Brünger et al., 1987). The structure of the K73H mutant enzyme was refined solely with X-PLOR. In either case, solvent molecules were added independently of the crystal structure of the native protein.

The interactive graphics programs FRODO (Jones, 1985), running on an E&S PS390 system, and TURBO-FRODO (Roussel & Cambillau, 1989), running on a Silicon Graphics INDIGO2 workstation, were used for map inspection and model modification of the S70A and K73H mutant structures, respectively.

**Binding Studies in the Crystals.** The soaking experiments and cryocrystallographic studies followed a protocol similar to that described previously (Chen & Herzberg, 1992). Prior to soaking with clavulanate or ampicillin solutions, the crystals were equilibrated overnight in solutions containing 80% saturated ammonium sulfate and 100 mM sodium bicarbonate at pH 8.0. Next, the crystals were transferred to a similar solution that also contained the desired  $\beta$ -lactam compound. For each antibiotic, a number of experiments were carried out, varying the  $\beta$ -lactam concentration and the soaking period. The following condition provided the best results: A crystal of the S70A mutant enzyme was soaked for 2.5 h in a solution containing 1.3 mM ampicillin (approximately 1600-fold molecular excess as estimated from

Table 2:  $k_{\text{cat}}$  Values ( $\text{s}^{-1}$ )

enzyme	benzylpenicillin	nitrocefin
wild-type	141.0	15.5
S70A <sup>a</sup>	$2.4 \times 10^{-3}$	$4.9 \times 10^{-4}$
S70A <sup>b</sup>	$2.0 \times 10^{-4}$	$1.2 \times 10^{-4}$
K73H	undetectable	$1.6 \times 10^{-4}$

<sup>a</sup> Enzyme expressed in *S. aureus*. <sup>b</sup> Enzyme expressed in *E. coli*.

the crystal volume and soaking solution volume). A second crystal was soaked for 1 h in 19 mM clavulanate (56 000-fold molecular excess). The K73H  $\beta$ -lactamase crystal was soaked for 4 h in 2 mM ampicillin solution (1000-fold excess). The concentration of ampicillin was lower than that of clavulanate because of its lower solubility in 80% saturated ammonium sulfate solution. Each crystal was picked up and coated with a layer of a 1:1 mixture of immersion oil (Banco) and Paratone-N oil (Exxon). Flash-freezing at approximately 120 K was achieved with a modified Enraf-Nonius FR558 liquid nitrogen cryostat. As with the crystals of the native enzyme (Chen & Herzberg, 1992), the freezing resulted in a dramatic reduction of the b unit cell dimension (Table 1). Therefore the starting model for the refinement was that of the native enzyme determined at 120 K, but with Ser70 omitted.

## RESULTS AND DISCUSSION

**Kinetic Characterization.** The activities of the two mutant  $\beta$ -lactamases are much impaired (Table 2), although the rates of  $\beta$ -lactam hydrolysis still represent between  $10^3$ - and  $10^4$ -fold acceleration over the nonenzymatic reaction (Gensmantel et al., 1978). The S70A enzyme exhibits linear progress curves for the hydrolysis of both benzylpenicillin and nitrocefin, with catalytic rates that are reduced by 4–5 orders of magnitude compared with the wild-type enzyme. Similar low rates have been observed for the hydrolysis of nitrocefin by the K73H mutant enzyme, whereas the hydrolysis of benzylpenicillin could not be detected at all. Because of the low rates, the  $K_m$  values were not measured, and only  $k_{\text{cat}}$  values are provided (Table 2).

The kinetic rates of nitrocefin hydrolysis by K73H  $\beta$ -lactamase were measured as a function of pH in the range between 5 and 8, with the anticipation that if increased rates were observed, this would provide information about the  $pK_a$  of the histidine. Four series of experiments have been carried out on different dates. In all cases, the  $k_{\text{cat}}$  values remained within the  $10^{-4} \text{ s}^{-1}$  range, showing that the pH change does not lead to significant recovery of activity. Thus, either the protonation state of His73 remains the same within the pH range or the impaired activity of the enzyme is not related to the protonation state of the histidine. The crystal structure helps clarify this issue.

Table 3: Refinement Statistics

	S70A	S70A+AmpC <sup>a</sup>	K73H
resolution range, Å	8.0–2.1	8.0–2.0	8.0–1.9
no. unique reflections, $F \geq 2\sigma(F)$	14361	16371	19308
<i>R</i>	0.170	0.171	0.168
no. of amino acid residues	257	257	258
no. of water molecules	161	426	177
no. of sulfate ions		3	
rms deviations from ideal geometry			
bond length (Å)	0.020	0.021	0.017
bond angles (deg)	1.9	2.1	1.8

<sup>a</sup> Abbreviations: AmpC, ampicillin.

**Refinement Results.** The refined structure of the S70A  $\beta$ -lactamase includes 257 amino acid residues and 161 solvent molecules. The final *R*-factor is 0.170 ( $R = \sum_h |F_o| - |F_c| / \sum_h |F_o|$ , where  $|F_o|$  and  $|F_c|$  are the observed and calculated structure factor amplitudes, respectively) for 14 361 reflections in the resolution range 8.0–2.1 Å for which  $F \geq 2\sigma(F)$  (Table 3). The model of the K73H  $\beta$ -lactamase consists of 258 amino acid residues (including an N-terminal methionine that was inserted for expression in *E. coli*) and 177 solvent molecules. The *R*-factor is 0.168 for 19 308 reflections in the range 8.0–1.9 Å for which  $F \geq 2\sigma(F)$ . The stereochemical parameters are well within the range known from the crystal structures of small peptides (Table 3). The electron density maps associated with the sites of mutations are shown in Figure 1.

Refinement of the structure of the S70A mutant enzyme soaked with ampicillin was carried out to a final *R*-factor of 0.171 for 16 873 reflections within the resolution range 8.0–2.0 Å for which  $F \geq 2\sigma(F)$ . Because this was a flash-frozen crystal, the quality of the electron density is excellent. The coordinate set includes 257 amino acid residues of which 10 have been modeled with 2 alternate side-chain conformations, 426 solvent molecules, and 3 sulfate ions. Residual density was observed in the active site, yet it was not sufficiently clear to account for a complete atomic model of ampicillin (Figure 2a). The data of the clavulanate-soaked crystal were partially refined to a *R*-factor of 0.259. Here again, the residual density in the active site was not clear enough for developing a detailed model of the bound inhibitor; thus, the refinement was not completed. The difference electron density in the active site was quite similar to that of the ampicillin-soaked crystal (Figure 2b). Finally, initial refinement of the diffraction data for the K73H mutant enzyme soaked with ampicillin followed by difference Fourier calculation did not reveal any electron density indicative of a bound ampicillin. Thus, refinement was not pursued.

**Structure and Function of S70A  $\beta$ -Lactamase.** Within the accuracy expected at the resolution of the structure determination, the overall structure of the S70A  $\beta$ -lactamase is identical to that of the native enzyme. When the coordinates of the two models are superimposed, the root-mean-square (rms) deviation is 0.2 Å for the  $\alpha$ -carbon atoms and 0.3 Å for all atoms. The superposition shows that, with the exception of the missing hydroxyl group at position 70, the active site environments are identical within experimental error (Figure 3). Therefore, the dramatic drop in the turnover number for both benzylpenicillin and nitrocefin may be attributed to the elimination of the protein nucleophilic group,

the O' atom of Ser70. Mistranslation that leads to production of wild-type enzyme must be considered as well. Mechanism-based inhibition of such a revertant of the S70A mutant enzyme from *S. albus G* has shown that this occurs with low frequency (Jacob et al., 1991). For the *S. aureus* mutant enzyme, the residual activity is even lower, although it still represents some 1000–10 000-fold acceleration relative to the nonenzymatic hydrolysis. That the activity is not completely abolished is not unexpected if the example of the catalytic serine of subtilisin replaced by an alanine (S221A) is considered (Carter & Wells, 1988). These authors observed an even more dramatic, millionfold, drop in turnover number. They proposed that the residual activity may be derived from the remaining binding determinants that stabilize the transition state complex. Similar arguments may be advanced to explain the kinetics of the S70A  $\beta$ -lactamase.

With the elimination of the catalytic serine, the turnover number is so low that one would anticipate the possibility of trapping enzyme–substrate Michaelis complexes in the crystal, given the soaking periods and excess  $\beta$ -lactam concentrations used. The electron density corresponding to the solvent region in the active site has been compared with that of the native structure determined at 120 K (Chen et al., 1992). While the density peaks in the native map are consistent with discrete sites of water molecules, the buildup of density in the substrate-soaked crystals is continuous, indicating the binding of a molecule larger than water (Figure 2). Nevertheless, neither ampicillin nor clavulanate formed complexes that were sufficiently tight to reveal the atomic details of the molecules. The possibility that competition with the sulfate ions (present in the crystallization solutions at approximately 3.3 M concentration) could reduce the affinity of the substrate has been examined by determining the dependence on ammonium sulfate concentration of the  $K_m$  value of ampicillin hydrolysis by the wild-type enzyme. Within the salt saturation range of 0–60%, no significant trend was observed. The  $K_m$  values were  $33 \pm 3 \mu\text{M}$ ,  $55 \pm 3 \mu\text{M}$ , and  $46 \pm 4 \mu\text{M}$  for 0%, 30%, and 60% saturated ammonium sulfate, respectively. Hence, it is not likely that the lack of tight  $\beta$ -lactam binding to the mutant  $\beta$ -lactamase arises from competition with sulfate.

**Structure and Function of K73H  $\beta$ -Lactamase.** With the exception of the three N-terminal residues, the overall fold of K73H  $\beta$ -lactamase is essentially the same as that of the native enzyme. The density associated with the added methionine residue at the N-terminus of K73H  $\beta$ -lactamase (numbered Met30) and with the following two residues indicates that the main-chain conformation of Met30-Lys31-Glu32 is helical, in contrast to the native structure, where the first residue of the helix is Glu32. Starting at residue 33, the rms deviation in the  $\alpha$ -carbon atoms between the native and mutant molecules is 0.2 Å. For all the atoms (also excluding Lys177 which adopts a different side-chain conformation in each of the structures such that the distance between the respective amino groups is 7.5 Å), the rms deviation is 0.3 Å. Most side-chain positions that deviate from those of the native structure by more than 1 Å correspond to surface lysine residues with high crystallographic temperature factors. Otherwise, the only significant deviation in side-chain conformation is that of the catalytic serine residue (Figure 4). Obviously, the change is induced because of the proximity to the mutated residue.

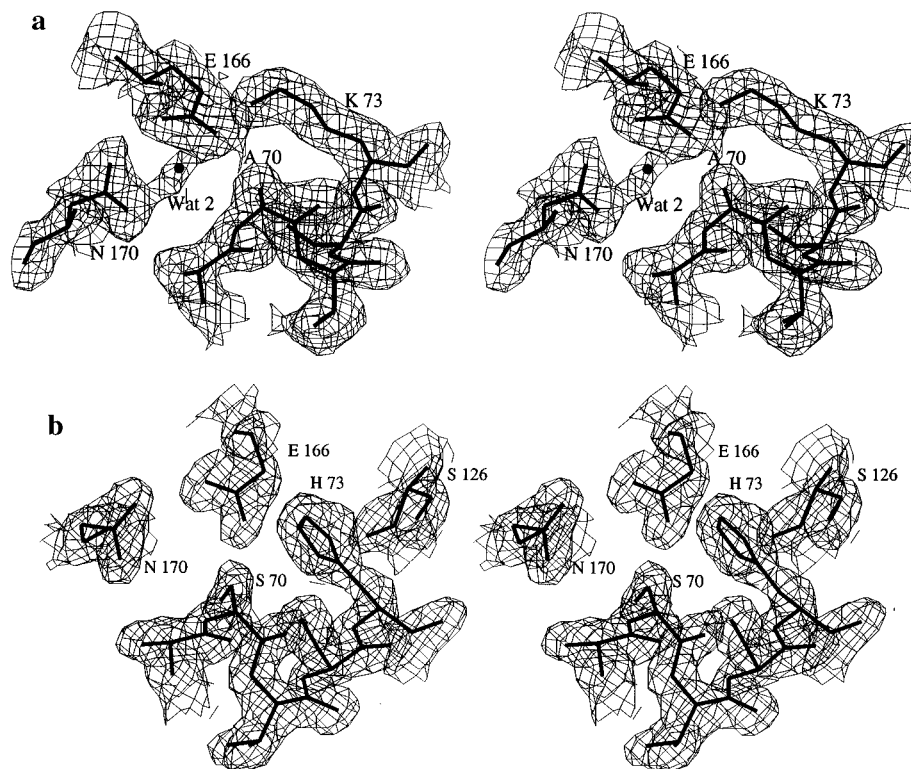


FIGURE 1: Stereoscopic representation of the electron density maps in the regions of the mutations, displayed together with the protein model. The maps are calculated with the coefficients  $2F_o - F_c$  and contoured at the  $1\sigma$  level. (a) S70A  $\beta$ -lactamase. (b) K73H  $\beta$ -lactamase.

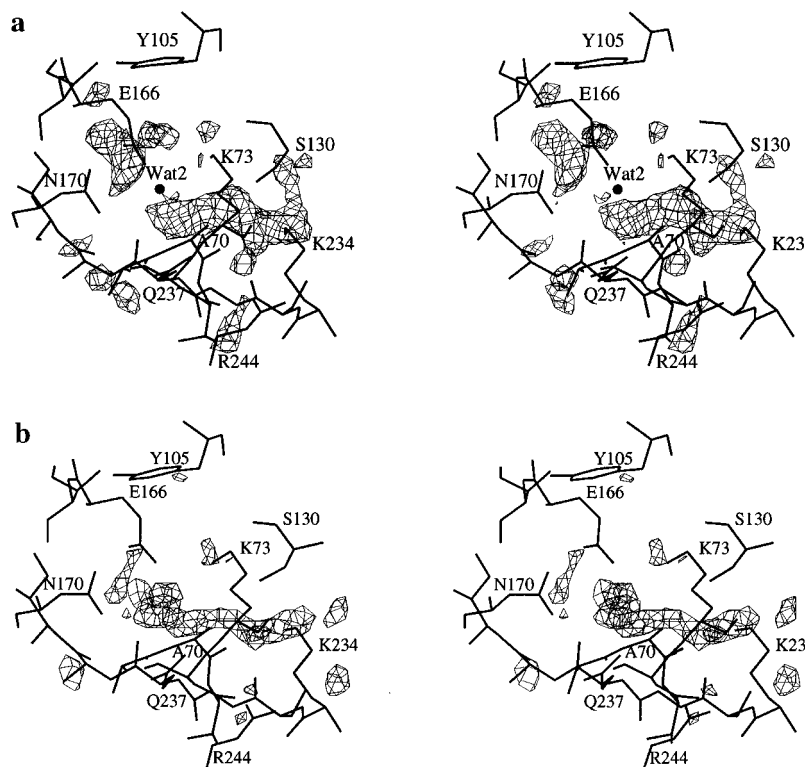


FIGURE 2: Stereoscopic representation of the difference electron density maps in the region of the active site of the S70A  $\beta$ -lactamase crystals soaked with  $\beta$ -lactams and flashed-frozen. The coefficients  $F_o - F_c$  and calculated phases are used, and the maps are contoured at the  $2.5\sigma$  level. (a) Soaking with ampicillin. The final map at the end of the refinement is shown. Solvent molecules have been included in the structure factor calculation, but no substrate model. (b) Soaking with clavulanate. The structure factors were calculated after initial refinement, and include only the protein model and no solvent molecules.

To the extent possible, His73 follows the trace of the lysine residue of the native structure (Figure 4). The  $\chi^2$  dihedral angle of the histidine is close to  $180^\circ$ , a sterically strained conformation that is uncommon in protein crystal

structures. One notable perturbation is that the bulkier histidine ring displaces one of the buried water molecules that are observed in the native structure underneath the active site floor (Herzberg, 1991). The buried water molecules fill

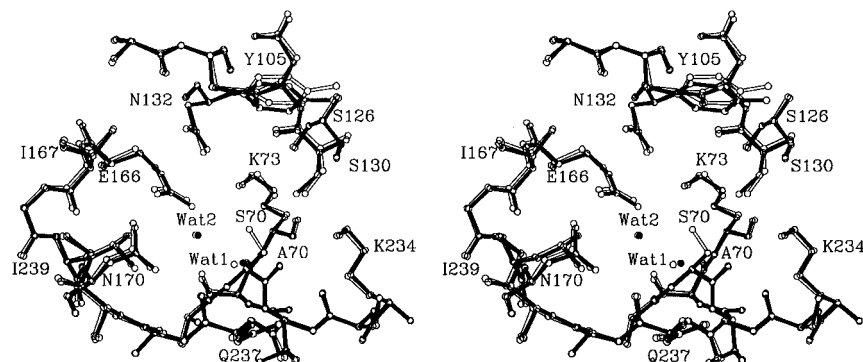


FIGURE 3: Stereoscopic view of the superposition of the active site regions of native and S70A  $\beta$ -lactamases. The oxyanion hole and the proposed deacylation water molecules are labeled Wat1 and Wat2, respectively.

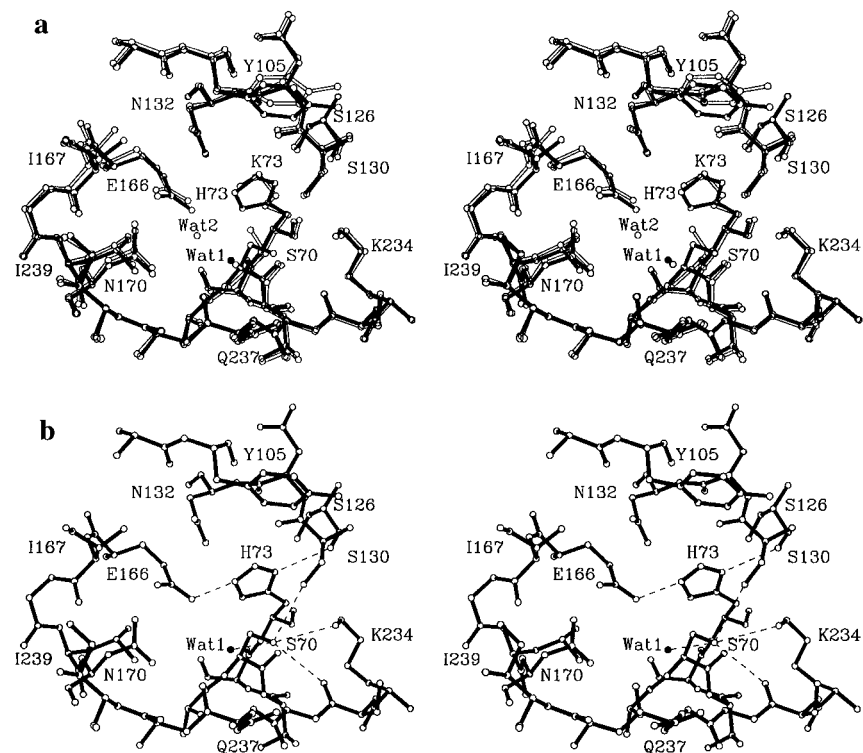


FIGURE 4: (a) Stereoscopic view of the superposition of the active site regions of native and K73H  $\beta$ -lactamases. (b) The active site of the K73H mutant enzyme, highlighting in dashed lines the electrostatic interaction associated with His73 and Ser70. The oxyanion hole and the proposed deacylation water molecules are labeled Wat1 and Wat2, respectively. Wat2 is not observed in the crystal structure of K73H  $\beta$ -lactamase.

empty space in the interior of the protein, but have no access to the active site. Therefore, no direct structural role is attributed to the displaced water molecule in substrate binding. Although nitrogen and carbon atoms cannot be discriminated at the resolution of the structure determination, the type of interactions formed between the histidine side-chain and the neighboring residues reveal which are the two nitrogen atoms: The  $N^{\delta}$  atom forms an electrostatic interaction with the carbonyl oxygen atom of Ser126 (3.1 Å), and the  $N^{\epsilon}$  atom forms an electrostatic interaction with Glu166 (2.6 Å). This indicates that His73 and Glu166 share a proton, and that the interaction occurs with charge separation (salt bridge). When compared with the native structure, the  $N^{\epsilon}$  atom is displaced by 1.6 Å from the position of the amino group of Lys73. Moreover, the orientation of the histidine ring is incompatible with favorable electrostatic interaction with the catalytic Ser70 as observed with Lys73 in the native structure. The consequence is that the side-chain of Ser70 adopts an alternative conformation such that the hydroxyl

group is oriented away from the histidine and toward the carbonyl oxygen atom of Ser235 (3.2 Å). It also forms electrostatic interactions with the amino group of Lys234 (3.3 Å), with Ser130 (3.2 Å), and with the water molecule that is located in the oxyanion hole (3.0 Å). In this conformation, the hydroxyl group of Ser70 is not poised for nucleophilic attack on substrate. Thus, if the arrangement observed in the crystal represents the predominant state of the enzyme in solution, the dramatic drop in activity should be attributed to both His73 and Ser70 dispositions.

Because of the alternate conformation of the Ser70 side-chain, the position of the  $C^{\beta}$  atom is displaced by 1 Å compared with the native structure, and the electrostatic interaction between the hydroxyl group and the proposed deacylation water molecule is eliminated (Figure 4a). If the water molecule was present also in the mutant enzyme, its distance to the  $C^{\beta}$  atom of Ser70 would be 2.8 Å, a much too short van der Waals contact. Indeed, no electron density is observed in the niche between Glu166 and Asn170; hence,

either the water molecule does not bind at all, or it does not occupy the site long enough to be observed crystallographically. By contrast, the oxyanion hole is still occupied by a water molecule.

Modeling followed by energy minimization shows that the available space is sufficient for His73 to adopt a more commonly observed  $\chi^2$  dihedral angle while maintaining the native structure conformation of the Ser70 side-chain. In that conformation, the N $^{\epsilon}$  atom of the imidazole ring would interact electrostatically with the Ser70 O $^{\gamma}$ . The histidine in that case would not be necessarily charged, in contrast to the charged state implied by the crystallographically observed conformation. Also, the niche for the proposed deacylating water molecule would be restored.

Could the experimentally observed conformations together with the model of the alternative conformations of His73 and Ser70 be used as a guide for ascertaining the charge state of Lys73 in the native enzyme? It is tempting to speculate that since the active site electrostatic environment in its unbound form supports a positively charged histidine, a lysine residue should also exist predominantly in the protonated state. The K73R mutant of the *B. cereus*  $\beta$ -lactamase, which retains substantial catalytic activity (Gibson et al, 1990), and the NMR data (Damblon et al., 1996) both suggest that a positive charge is preferred in this location. On the other hand, it may be argued that the observed interactions of the imidazole ring cannot be reproduced by a lysine side-chain; thus, the conjecture may be inappropriate. Moreover, the protonation state can change when the active site is desolvated upon substrate binding, and it is the electrostatics of the Michaelis complex that ultimately determine the mechanism of proton transfer. Further experiments are required to resolve this issue.

#### ACKNOWLEDGMENT

We thank Drs. Richard Novick, Noreen Murray, Richard Hayward, Edward Eisenstein, and Philip Bryan for gifts of strains, plasmids, and bacteriophages. We are grateful to Tim Foster for providing the method for electroporation of *S. aureus* and to Richard Hayward for much helpful advice. We also thank the Richard Lounsbery Foundation for the gift of a spectrophotometer.

#### REFERENCES

- Adachi, H., Ohta, T., & Matsuzawa, H. (1991) *J. Biol. Chem.* 266, 3186–3191.
- Amann, E., & Brosius, J. (1985) *Gene* 40, 183–190.
- Ambler, R. P. (1979) in *Beta-Lactamases* (Hamilton-Miller, J. M. T., & Smith, J. T., Eds.) pp 99–125, Academic Press, London.
- Ambler, R. P., Coulson, A. F. W., Frère, J.-M., Ghuysen, J.-M., Joris, B., Forsman, M., Levesque, R. C., Tiraby, G., & Waley, S. G. (1991) *Biochem. J.* 276, 269–270.
- Antosiewicz, J., McCammon, A., & Gilson, M. K. (1994) *J. Mol. Biol.* 238, 415–436.
- Brünger, A. T., Kuriyan, J., & Karplus, M. (1987) *Science* 235, 458–460.
- Carrey, E. A., & Pain, R. H. (1978) *Biochim. Biophys. Acta* 533, 12–22.
- Carter, P., & Wells, J. A. (1988) *Nature* 332, 564–568.
- Casadaban, M. J., & Cohen, S. N. (1980). *J. Mol. Biol.* 138, 179–207.
- Chen, C. C. H., & Herzberg, O. (1992) *J. Mol. Biol.* 224, 1103–1113.
- Close, T. J., & Rodriguez, R. L. (1982) *Gene* 20, 305–316.
- Coulson, A. (1985) *Biotechnol. Genet. Eng. Rev.* 3, 219–253.
- Escobar, W. A., Tan, A. K., & Fink, A. L. (1991) *Biochemistry* 30, 10783–10787.
- Finzel, B. C. (1987) *J. Appl. Crystallogr.* 20, 53–55.
- Gensmantel, N. P., Gowling, E., & Page, M. I. (1978) *J. Chem. Soc., Perkin Trans. 2*, 335–342.
- Gibson, R. M., Christensen, H., & Waley, S. G. (1990) *Biochem. J.* 272, 613–619.
- Hendrickson, W. A., & Konnert, J. H. (1980) in *Biomolecular Structure, Function, Conformation and Evolution* (Srinivasan, R., Ed.) Vol. I, pp 43–75, Pergamon Press, Oxford.
- Herzberg, O. (1991) *J. Mol. Biol.* 217, 701–719.
- Herzberg, O., & Moul, J. (1987) *Science* 236, 694–701.
- Herzberg, O., & Moul, J. (1991) *Curr. Opin. Struct. Biol.* 1, 946–953.
- Herzberg, O., Kapadia, G., Blanco, B., Smith, T., & Coulson, A. F. W. (1991) *Biochemistry* 30, 9503–9509.
- Ho, S. N., Hunt, H. D., Horton, R. M., Pullen, J. K., & Pease L. R. (1989) *Gene* 77, 51–59.
- Howard, A. J., Gilliland, G. L., Finzel, B. C., Poulos, T., Ohlendorf, D. O., & Salemme, F. R. (1987) *J. Appl. Crystallogr.* 20, 383–387.
- Jacob, F., Joris, B., & Frère, J. M. (1991) *Biochem. J.* 277, 647–652.
- Jelsch, C., Lenfant, F., Masson, J. M., & Samama, J. P. (1992) *FEBS Lett.* 299, 135–142.
- Jelsch, C., Mourey, L. F., Masson, J. M., & Samama, J. P. (1993) *Proteins: Struct., Funct., Genet.* 16, 364–383.
- Jones, T. A. (1985) *Methods Enzymol.* 115, 157–171.
- Knowles, J. R. (1985) *Acc. Chem. Res.* 18, 97–104.
- Knox, J. R., & Moews, P. C. (1991) *J. Mol. Biol.* 220, 435–455.
- Kreiswirth, B., Lofdahl, S., Betley, M. J., O'Reilly, M., Schlievert, P. M., Berdoll, M. S., & Novick, R. P. (1983) *Nature* 305, 709–712.
- Lamotte-Brasseur, J., Dive, G., Dideberg, O., Charlier, P., Frère, J.-M., & Ghuysen, J.-M. (1991) *Biochem. J.* 279, 213–221.
- Lobkovsky, E., Billing, E. M., Moews, P. C., Rahil, J., Pratt, R. F., & Knox, J. R. (1994) *Biochemistry* 33, 6762–6772.
- Moews, P. C., Knox, J. R., Dideberg, O., Charlier, P., & Frère, J.-M. (1990) *Proteins: Struct., Funct., Genet.* 7, 156–171.
- Monnaie, D., Dubus, A., & Frère, J. M. (1994) *Biochem. J.* 302, 1–4.
- Moul, J., Sawyer, L., Herzberg, O., Jones, C. L., Coulson, A. F. W., Green, D. W., Harding, M. M., & Ambler, R. P. (1985) *Biochem. J.* 225, 167–176.
- Roussel, A., & Cambillau, C. (1989) *Silicon Graphics Geometry Partners Directory*, pp 77–78, Silicon Graphics, Mountain View, CA.
- Smith, T. J. (1992) Ph.D. Thesis, University of Edinburgh.
- Strynadka, N. C. J., Adachi, H., Jensen, S. E., Johns, K., Sielecki, A., Betzel, C., Sutoh, K., & James, M. N. G. (1992) *Nature* 359, 700–705.
- Tsukamoto, K., Tachibana, K., Yamazaki, N., Ishii, Y., Ujii, K., Nishida, N., & Sawai, T. (1990) *Eur. J. Biochem.* 188, 15–22.
- Wang, P.-Z., & Novick, R. P. (1987) *J. Bacteriol.* 169, 3082–3087.
- Zawadzke, L. E., Smith, T., & Herzberg, O (1995) *Protein Eng.* 8, 1275–1285.